High-Contrast Electroswitching of Emission and Coloration Based on Single-Molecular Fluoran Derivatives

ARTICLE *in* THE JOURNAL OF PHYSICAL CHEMISTRY A · JULY 2014

Impact Factor: 2.69 · DOI: 10.1021/jp5060588 · Source: PubMed

3 AUTHORS:

Kenji Kanazawa
Chiba University
8 PUBLICATIONS **49** CITATIONS
SEE PROFILE

Kazuki Nakamura
Chiba University
57 PUBLICATIONS **659** CITATIONS
SEE PROFILE

Norihisa Kobayashi
Chiba University
117 PUBLICATIONS **1,525** CITATIONS
SEE PROFILE

THE JOURNAL OF PHYSICAL CHEMISTRY A

Article

pubs.acs.org/JPCA

High-Contrast Electroswitching of Emission and Coloration Based on Single-Molecular Fluoran Derivatives

Kenji Kanazawa, Kazuki Nakamura,* and Norihisa Kobayashi*

Department of Image and Materials Science, Graduate School of Advanced Integration Science, Chiba University, 1-33 Yayoi-cho, Inage-ku, Chiba 263-8522, Japan

Supporting Information

ABSTRACT: Multifunctional electroswitching of both emission and coloration was demonstrated by using fluoran derivatives in an electrolytic solution. Further, in order to investigate changes in the photophysical properties induced by electrical stimuli, we measured cyclic voltammogram, absorption spetra, emission spectra, and molecular orbital calculation. The mechanism for this electroswitching was attributed to the reversible electrochemically induced closing and opening of the lactone ring in the fluoran molecule. All neutral fluoran molecules were colorless and did not exhibit any fluorescence, while the oxidized (lactone ring-opened form) molecule was yellow and displayed a green fluorescence as a consequence of the extended, planar, conjugated system. Furthermore, this fluoran molecule achieved reversible electroswitchable emission and coloration with high on/off contrast.

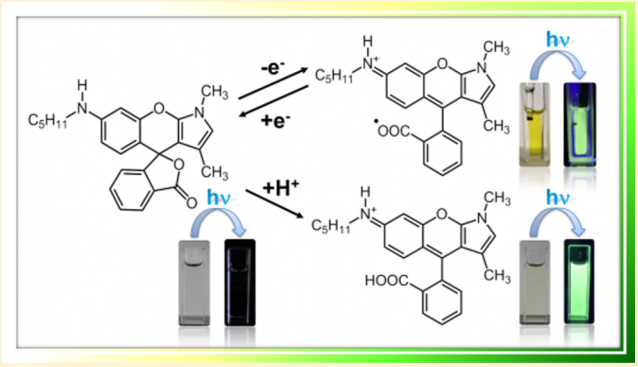

INTRODUCTION

Multifunctional molecular switches exhibiting changes in both emission and coloration in response to various external triggers such as thermal, photo, and electric stimuli have attracted much attention for potential application as chemical sensors,[1,2] biochemical labels,[3] molecular logic gates,[4−6] molecular memories,[7,8] and display devices.[9−12] Various thermosensitive multifunctional materials showing tunable emission and/or coloration have been developed by using the phase transitions of liquid crystals,[13,14] the changes in the conformation of organic and inorganic compounds,[15−17] and the fluoran dye-developer system.[18,19] Photoresponsive multifunctional systems that show both tunable emission and coloration have also been reported previously; these systems consist of a photochromic diarylethene derivative associated with a luminescent moiety.[20−22] In fluorophore−diarylethene systems, turn-on/turn-off fluorescence occurs; the initial fluorescent open-ring isomer is switched off during diarylethene photocyclization, and closed-ring isomers show very weak fluorescence due to intramolecular energy or electron transfer from the fluorophore to the closed-ring diarylethene. The fluorescence can be readily restored by irradiating the system with visible light.

We are focusing on electrical stimuli to activate multifunctional molecules because such stimuli can be applied rapidly, remotely, and reversibly while maintaining the mild conditions suitable for biological systems.[23−26] Previously, we electrochemically switched the emission and absorption of multifunctional systems fabricated by integrating a luminescent europium(III) complex and an electrochemically active material, diheptyl viologen and/or prussian blue.[27−30] The fluorescence switching in our systems was induced by intermolecular energy transfer between fluorescent and electrochemically active molecules in response to electrical stimuli. Recently, considerable effort has been made to investigate electroswitchable photophysical properties by combining photoluminescent and electrochemically active molecules.[31,32] However, most of these systems, including ours, usually do not exhibit sufficiently quick response, high reversibility, and high contrast in the fluorescence response because long-term application of electrical stimuli is required to achieve such a response. Almost all previously reported multifunctional materials showing electrochemical switching of emission and absorption were prepared by simply mixing or stacking emission and coloration materials.

The emission- and coloration-related moieties must be covalently connected to improve the response and repetition stability, and those multifunctionalities should occur within the same molecule. Furthermore, we should also consider the distance between the fluorescent "donor" and chromic "acceptor" units to realize the efficient electron and related energy transfer from the highest occupied molecular orbital (HOMO) to the lowest unoccupied molecular orbital (LUMO) level of each molecule unit.[27−30,33−35]

Received: June 18, 2014
Revised: July 15, 2014

dx.doi.org/10.1021/jp5060588 | J. Phys. Chem. A XXXX, XXX, XXX−XXX

Herein, we describe the electroswitching of the emission and coloration of single-molecular fluoran derivatives. Fluoran molecules, which exhibit reversible vivid color change with quite high repetition stability by interacting with electron acceptors (e.g., phenol formaldehyde resins and bisphenol), are widely used in a variety of applications, such as pressure-sensitive and thermosensitive recording paper systems.[36−38] Yamauchi et al. used a mesoporous TiO_2 electrode to induce reversible electrochemical color change of fluoran compounds and reported the changes in color with response on a time scale of several milliseconds, high resolution, and high repetition stability (over 10 000 cycles).[39]

In this study, we demonstrated reversible electrochemically induced high-contrast switching of the emission and coloration of fluoran molecules associated with changes in the intramolecular structure (Scheme 1). Unlike the viologen−europium(III) system, emission and coloration are controlled simultaneously through the electrochemical- or protonation-induced closing and opening of the lactone ring in the fluoran molecule: Neutral fluoran molecules were colorless and did not show any fluorescence because the lactone ring was closed, while protonated and oxidized fluoran molecules were yellow and showed a green emission because of the extended conjugation resulting from cleavage of the lactone ring (Scheme 1). Moreover, we combined density functional theory (DFT) and time-dependent DFT (TD-DFT) to study the switching of the emission and coloration mechanism.

Scheme 1. Schematic Illustration of Electrochemical Switching of Fluoran Emission between the Neutral and Oxidized State

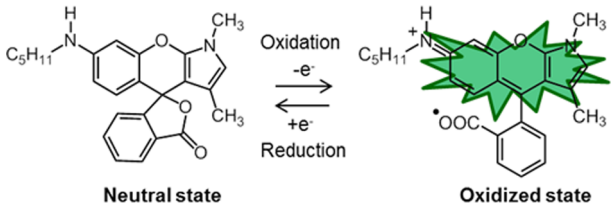

EXPERIMENTAL SECTION

Materials. Yellow-1 (fluoran molecule: see Scheme 1 for the chemical structure) was provided by Yamada Kagaku Co. Ltd. Propylene carbonate (PC) (Kanto Chemical Co. Inc.) was used as a solvent after removing water with use of molecular sieves. Sulfuric acid (H_2SO_4) and ferrocene (Fc) were purchased from Kanto Chemical Co. Inc. and used as received. Tetra-*n*-butylammonium perchlorate (TBAP) (Kanto Chemical Co. Inc.) was used as supporting electrolyte without further purification.

Electrochemical Measurements. Cyclic voltammograms (CVs) and chronoamperometric measurement were recorded on a potentiostat/galvanostat (ALS, 660A) equipped with a computer. A three-electrode cell was constructed with an indium tin oxide (ITO) glass electrode (reaction area of electrode was 2 cm^2) as the working electrode, a Pt wire as the counter electrode, and a Ag/Ag^+ electrode as the reference electrode. The scan rate was 50 mV/s. Absorption spectra were recorded in situ during the application of a potential between 1.1 and −1.2 V (vs Ag/Ag^+) with use of a diode array detection system (Ocean Optics, USB2000). The solution for electrochemical studies was prepared by dissolving fluoran (5 mM) and TBAP (50 mM) in PC. The solution was purged with nitrogen gas for 20 min before each experiment.

Photophysical Measurements. Ultraviolet−visible (UV−vis) absorption spectra for the cells were measured with a spectrophotometer (JASCO, V-570) and quartz cells whose paths were 1.0 cm long. Photoluminescence spectra were obtained with a spectrofluorometer (JASCO, FP-6600) and a three-electrode cell containing fluoran molecules (5 mM) and TBAP (50 mM) in PC. The excitation wavelengths for the neutral and oxidized samples were 300 and 450 nm, respectively. Fluorescence quantum yields and time-resolved fluorescence decay for the solution were investigated by dissolving fluoran (1 μM) in PC with or without H_2SO_4 (10 μM). Fluorescence quantum yields of sample were recorded on a Quantaurus-QY (Hamamatsu Photonics Co., C11347). Time-resolved fluorescence decay was measured by employing the time-correlated single-photon counting method and with use of an IBH-5000U instrument. A HORIBA JOBIN-YBON IBH 370 nm NanoLED instrument whose full width at half-maximum (fwhm) was 1.3 ns and whose repetition rate was 1 MHz was used to excite the samples. The obtained data were fit by using the IBH DAS6 fluorescence decay analysis software. The solution used for the optical measurements was purged with nitrogen gas for 20 min before each measurement.

Computational Method. The Gaussian 09 program package (Revision A.02)[40] and Kohn−Sham DFT[41−44] based on the Becke's three-parameter hybrid functional RB3LYP[45−48] with the 6-31G(d)[49] and 6-31+G(d) basis set were used to optimize the molecular geometries of the neutral and protonated fluoran molecules. Each optimization was verified by using frequency analysis. The frontier molecular orbital (FMO) energy levels were calculated by using the optimized structures. TD-DFT[50−52] was used with RB3LYP/6-31G(d) and RB3LYP/6-31+G(d) to stimulate the vertical transitions of the first 24 states of the neutral and protonated molecules, respectively. In all cases, solvent effects were simulated by employing a polarizable continuum model (PCM) with dimethyl sulfoxide (DMSO) as the solvent because the dielectric constant of DMSO (ε = 46.826) is the nearest to that of PC (ε = 66.1) in the PCM aprotic organic solvent.[53,54] Molecular orbitals were depicted by Gauss View 5.0 software.

RESULTS AND DISCUSSION

Electrochemical Properties. CVs (Figure 1a), changes in absorbance (Figure 1b), chronoamperometric response and time-dependent absorption at 465 nm (Figure 1c) were measured by using a three-electrode cell containing fluoran molecule (5 mM) and TBAP (50 mM)/PC electrolyte to investigate the electrochromic properties of the fluoran molecule. During potential sweep from 0 V to the positive direction, the CV for the solution showed one oxidation peak at 1.0 V (vs Ag/Ag^+). Further, in the case of continuous sweeping of the potential from 1.1 V to negative direction, one corresponding reduction peak was observed at −1.08 V. In contrast, when potential sweep was started from 0 V to negative direction, the CV for the solution did not show any reductive peak. Therefore, the electrochemical reaction of the fluoran molecule is based on the reaction not between neutral and reduced state but between neutral and oxidized state. The broad absorption bands with the peak around 465 nm increased when an oxidation potential of 1.0 V was applied for 5 s, resulting in a change in the color from transparent to yellow (Figure 1b,c). The absorption spectra of the oxidized fluoran

dx.doi.org/10.1021/jp5060588 | J. Phys. Chem. A XXXX, XXX, XXX−XXX

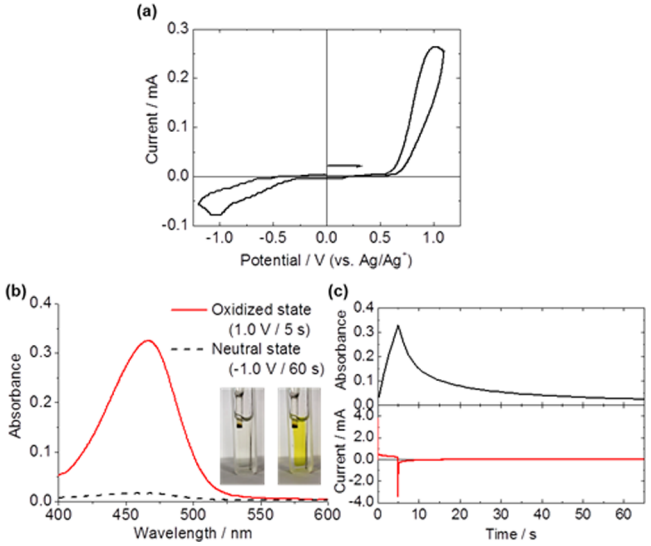

Figure 1. (a) CVs (scan rate at 50 mV/s) and (b) absorption spectra for the fluoran molecule-based EC solution. The insets show the photographs of EC-solution-based coloration changes of the fluoran molecule. (c) Time-dependent absorbance change at 465 nm (top) and chronoamperometric curve (bottom) recorded by stepping the applied potential between 1.0 and −1.0 V (vs Ag/Ag^+) for 5 and 60 s, respectively.

molecules (oxidized by applying 1.0 V for 5 s, Figure 1b) and those of the protonated one (protonated by adding H_2SO_4) were very similar (Figure S1 in the Supporting Information). Therefore, this increase in absorption bands at around 465 nm was due to the lactone ring opening induced extended π-conjugated system of the benzopyranopyrrole unit, as shown in Scheme 1. Furthermore, the absorption bands around 465 nm decreased to their initial value and the solution showed the color change from yellow to transparent when the reduction potential at −1.0 V was applied to the cell for 60 s (Figure 1b,c), indicating that the oxidized fluoran molecule recovered to its initial neutral state, as shown in Scheme 1. From data of chronoamperometric response and time-dependent absorbance change at 465 nm of the fluoran solution as shown in Figure 1c, we estimated the coloration efficiency (CE). CE is an important characteristic of electrochromic molecules. It is defined as the change in the optical density (ΔOD) for the charge consumed per unit electrode area (ΔQ) during the switching of the solution from neutral to oxidized state. The corresponding equation is given below:

$$\eta = \frac{\Delta \mathrm{OD}}{\Delta Q} = \frac{\Delta A}{\Delta Q} = \frac{A_o - A_n}{\Delta Q}$$

where A_o and A_n are the absorbance at 465 nm in oxidized and neutral states, respectively, and η denotes the CE. The CE of the fluoran molecule was measured as 392 $cm^2\ C^{-1}$ at 465 nm. This CE value is a relatively high value in comparison with those of other organic electrochromic molecules,[55−57] leading to high-contrast switching of coloration.

Photophysical Properties. Emission spectra for the fluoran molecule solution were monitored when an electrical potential was applied to the cell in order to investigate how the electrochemical reaction affected the emission (the measurement setup is shown in Figure 2a). Emission spectra for the fluoran molecules were monitored by using the cell shown in Figure 2a under conditions that prevented scattered light from

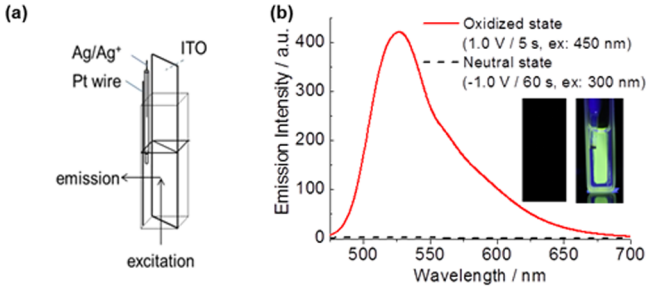

Figure 2. Schematic representation of measurement configuration of the fluorescence spectroelectrochemical cell and (b) emission spectra for the cell irradiated with UV light (450 or 300 nm) in the oxidized state (1.0 V for 5 s, red line) and neutral state (−1.0 V for 60 s, black dotted line). The insets are photographs of changes in fluorescence corresponding to the EC reaction.

the ITO electrode to be detected. Figure 2b shows emission spectra for the oxidized (1.0 V for 5 s, red line) and neutral (−1.0 V for 60 s, black dotted line) fluoran molecules subjected to photoexcitation at 450 and 300 nm, respectively. No emission was observed before the potential was applied to the cell. However, an emission band appeared at 465 nm (red line in Figure 2b) when an oxidation potential of 1.0 V (vs Ag/Ag^+) was applied to the cell for 5 s (Figure 2b, inset). Furthermore, the emission of fluoran molecules was quenched when the reduction potential of −1.0 V was applied to the cell for 60 s (black dotted line in Figure 2b), because applying the reduction potential induced the structural change from oxidized fluoran molecules to their original neutral state. The emission spectrum for the solution containing fluoran molecules protonated with H_2SO_4 also showed the green photoluminescence (Figure S2, Supporting Information) whose spectra was almost the same as electrochemically induced photoluminescence. The emission quantum yield and lifetime of the protonated fluoran molecules in the H_2SO_4/PC solution were 0.76 and 4.0 ns, respectively, as summarized in Figure S3 and Table S1, Supporting Information. Moreover, the radiative and nonradiative rate constants were calculated by using the following equations:

$$\phi = \frac{k_r}{k_r + k_{nr}}$$

$$\tau = \frac{1}{k_r + k_{nr}}$$

where ϕ, τ, k_r, and k_{nr} represent the emission quantum yield, emission lifetime, and radiative and nonradiative rate constants for the protonated fluoran molecule, respectively. The estimated radiative and nonradiative rate constants were 1.89 × 10^8 and 6.00 × 10^7 s^{-1}, respectively, indicating that the emission from the protonated fluoran molecules is not phosphorescence but fluorescence.

Electrochemical Switching of Emission and Coloration. Figure 3 shows the changes in the absorption at 465 nm and emission at 525 nm for the fluoran molecules when 1.0 and −1.0 V were consecutively applied to the cell for 5 and 60 s, respectively. The emission intensity and the absorbance rapidly increased because the fluoran molecules electrochemically oxidized within 5 s when 1.0 V potential was applied to the cell and was subsequently slowly decreased, and reverted to the initial intensity because the oxidative species was reduced when −1.0 V was applied to the cell for 60 s. This significant emission-coloration switching showed good reversibility due to

dx.doi.org/10.1021/jp5060588 | J. Phys. Chem. A XXXX, XXX, XXX−XXX

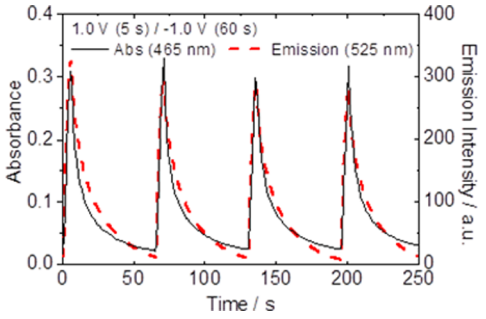

Figure 3. Change in absorbance at 465 nm (black line) and emission intensity at 525 nm (red dotted line) for the fluoren-molecule EC-solution-based cell. Potential step was 1.0 V for 5 s and −1.0 V for 60 s. Excitation wavelength was 450 nm.

the stability of the ring-opening and -closing structure of the ring in the fluoran molecule.

Mechanisms for Photophysical Switching Elucidated through Changes in Molecular Structure. We then estimated the energies of the HOMO and LUMO (given in Table 1) to elucidate the mechanisms for emission and

Table 1. Electrochemical Properties and Bandgap Energies of Neutral and Oxidized Fluoran Molecules

fluoran	E_{ox} [V][a]	E_{red} [V][a]	HOMO [eV]	LUMO [eV]	E_g [eV]
neutral	0.61		−5.35[b]	−1.07[c]	4.28[d]
oxidized		−0.35	−6.89[c]	−4.39[b]	2.50[e]

[a]Oxidation and reduction onset potentials determined from fluoran molecule vs Ag/Ag^+. [b]Calculated from equation HOMO (neutral state) or LUMO (oxidized state) = $[-(E_{ox}$ or $E_{red} - 0.06) - 4.8]$ eV in which 0.06 V is the half-wave potential of Fc/Fc^+ in PC and 4.8 eV is the energy level of Fc under vacuum. [c]LUMO (neutral state) = HOMO + E_g, HOMO (oxidized state) = LUMO − E_g. [d]Optical E_g in the neutral state is estimated by using the onset of absorption spectra. [e]E_g in the oxidized state is estimated from the point of intersection between absorption and emission spectra.

coloration controls through electrochemically induced change in the structure of the fluoran molecules. The HOMO energy level of the neutral fluoran molecules, which is the degree of ionization potential, and the LUMO energy level of the oxidized fluoran molecules, which is the degree of electron affinity, were estimated from the reference energy level of the half-wave potential of the Fc/ferrocenium (Fc^+) redox couple (4.80 eV under vacuum level), which was 0.06 V (vs Ag/Ag^+). E_{ox} (the oxidation onset potential) was 0.61 V (vs Ag/Ag^+) for the neutral fluoran molecules and E_{red} (the reduction onset potential) was −0.35 V (vs Ag/Ag^+) for the oxidized fluoran molecules. The LUMO level for the neutral fluoran molecules was also estimated relative to the corresponding HOMO level by using the optical band gap approximated by absorption edge in the absorption spectra (black line of Figure S1, Supporting Information). The HOMO level for the oxidized fluoran molecule was also obtained relative to the corresponding LUMO level by using the optical band gap approximated by intersection between absorption spectra and emission spectra of the fluoran molecule in the oxidized state (Figure S4, Supporting Information). The HOMO, LUMO, and HOMO−LUMO gap (E_g) of the fluoran molecule in each state were summarized in Table 1.

The molecular geometry was optimized based on DFT calculations with Gaussian 09 at the RB3LYP/6-31G(d) level for the neutral fluoran molecule and at the RB3LYP/6-31+G(d) level for the protonation-induced lactone ring opening structure, implying that these results were also applied to the electrochemically opened lactone rings of the protonated fluoran molecule because the corresponding absorption and emission spectra (optical properties) were consistent. All the solvent effects were simulated by using a PCM model with DMSO as the solvent. Figure 4 shows the FMOs of a neutral

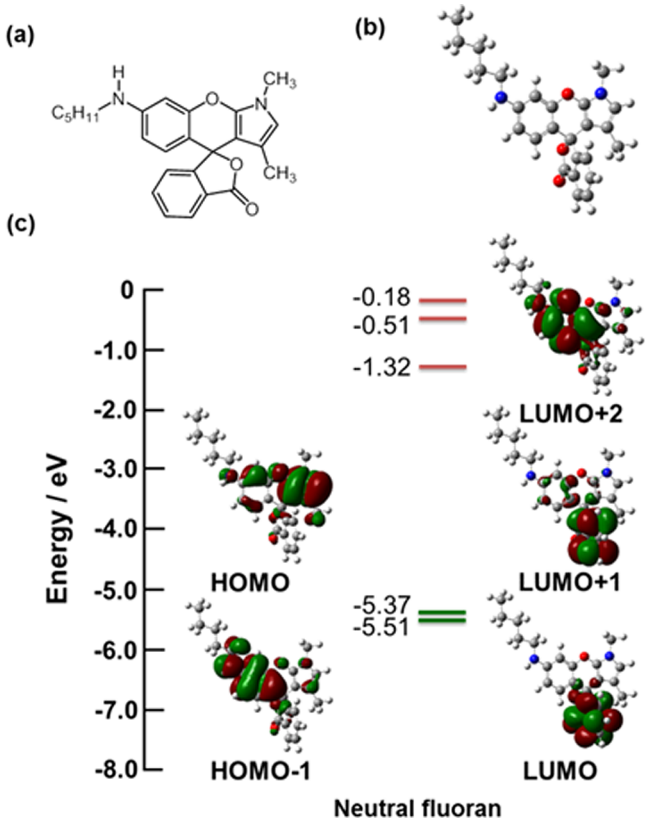

Figure 4. (a) Molecular structure, (b) optimized molecular structure, and (c) FMOs of neutral fluoran molecule calculated by RB3LYP/6-31G(d) DFT methods shown with corresponding relative energies. Key: C, gray; H, white; O, red; N, blue.

fluoran molecule, whose HOMO−1 and HOMO are mainly located on the benzopyranopyrrol ring and nitrogen atom in the molecule, indicating that the pyrrole or nitrogen unit/element in the molecule had oxidized, while the LUMO and LUMO+1 are predominantly located on the 1(3H)-isobenzofuranone ring in the molecule. In addition, the LUMO+2 is located on the benzopyran ring in the molecule. From the spread of these FMOs, fluoran-molecule quenching is possibly attributed to the lack of overlap between the HOMOs and LUMOs. The HOMO−LUMO gap for the neutral fluoran molecule is 4.05 eV (Figure 4), which is consistent with the experimentally obtained E_g (4.28 eV), as given in Table 1. This result suggests that the absorption bands are not in the visible range of the spectrum. TD-DFT and RB3LYP/6-31G(d) were used to simulate vertical transitions in order to validate the mechanism of emission property for the neutral fluoran molecule (Figure 5 and Table S2, Supporting Information). Figure 5 shows that the two spectra show similar shape such as the appearance of two intense absorption peaks in the ultraviolet region although the calculated absorption spectrum

dx.doi.org/10.1021/jp5060588 | J. Phys. Chem. A XXXX, XXX, XXX−XXX

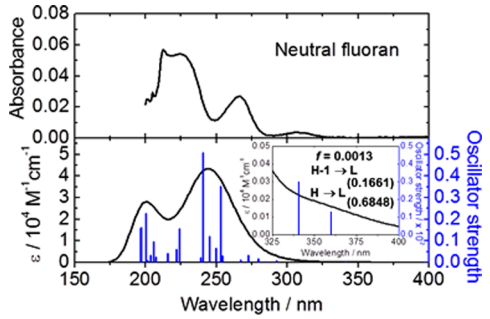

Figure 5. Absorption spectra for neutral fluoran molecule/PC solution (top) and calculated by using the TD-DFT method with PCM (RB3LYP-6-31G(d) basis set) for the same: blue bars indicate oscillator strength (bottom). The inset shows the close-up of the spectrum from 325 to 400 nm: f = oscillator strength, H = HOMO, L = LUMO, and other values are CI coefficients corresponding to the first transition band (360.05 nm).

(bottom) was blue-shifted by ~25 nm in comparison with the experimentally obtained one (top). The calculated excitation energy for the $S_0 \rightarrow S_1$ transition was 360.05 nm and the corresponding oscillator strength (f) was 0.0013 (absorption in DMSO), which was close to the experimental result (absorption in PC). The small f values (Table S2, Supporting Information) and the lack of overlap between either the HOMO−1 or HOMO and the LUMO (Figure 4) indicates that the transition from the ground state to the lowest lying excited one is strongly forbidden (Figure 5), i.e., the S_1 state is not directly accessible through photoexcitation. Instead of that, the S_1 state can only be populated through the internal conversion (IC) of higher allowed excited states such as S_5 (f = 0.0153), etc. (Table S2, Supporting Information).[58,59] According to Kasha's rule, IC quickly occurs, so S_5 will relax to S_1 before possibly relaxing to S_0.[58−64] Therefore, the lowest lying excited state, S_1, is nonemissive and will not radiatively decay to the ground state, S_0. (In this case, a nonradiative deactivation channel will act as a drain pipe for the excited-state energy.) This means that neutral fluoran molecules are probably nonfluorescent.

The LUMO, on the other hand, was localized in the benzopyranopyrrol ring of the molecule in the case of protonation-induced ring opening, as shown in Figure 6.

Furthermore, HOMO−1, HOMO, and LUMO were widely spread over the benzopyranopyrrol ring in the fluoran molecule and showed significant overlap, indicating that the experimentally observed emission from the oxidized fluoran molecule reflects the locally excited (LE) state. Moreover, the HOMO−LUMO, E_g, for the oxidized fluoran molecule was 3.27 eV (379 nm), as shown in Figure 6. Thus, the experimental and theoretical E_g values obtained for the oxidized fluoran molecule are smaller than those obtained for the neutral one as given in Table 1 and Figure 4, leading to the appearance of absorption bands in the visible range of the spectrum (Figure S2, Supporting Information). As in the case of the neutral fluoran molecule, TD-DFT and RB3LP/6-31+G(d) were used to simulate vertical transitions in order to validate the mechanism of emission control for the protonated fluoran molecule (Figure 7 and Table S3, Supporting Information). Figure 7 shows that the calculated (bottom) and experimentally obtained (top) absorption spectra also were generally consistent although the positions of two absorption peaks in the calculated spectrum were more blue-shifted than their counterparts in the

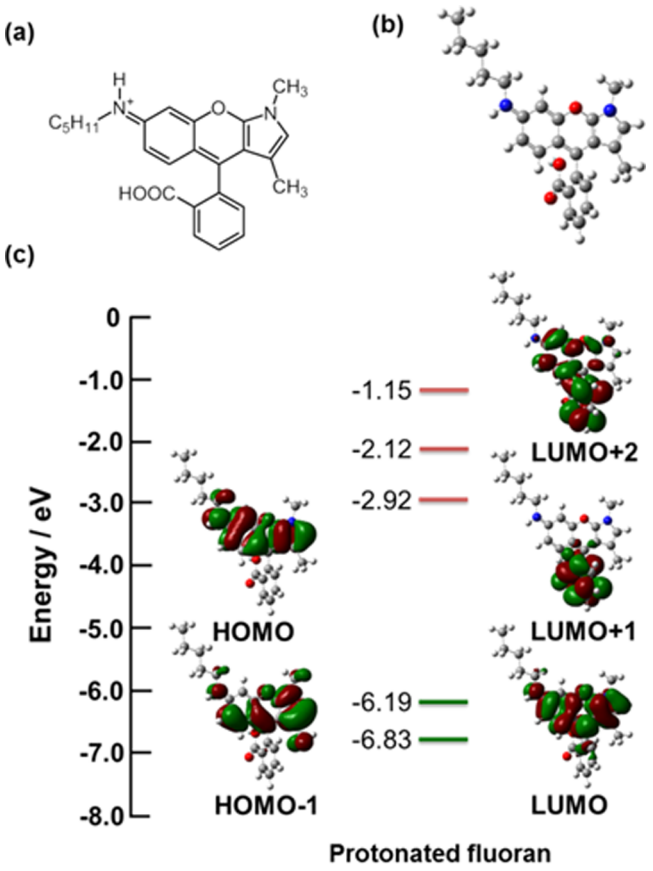

Figure 6. (a) Molecular structure, (b) optimized molecular structure, and (c) FMOs of the protonated fluoran molecule calculated by RB3LYP/6-31+G(d) DFT methods shown with corresponding relative energies. Key: C, gray; H, white; O, red; N, blue.

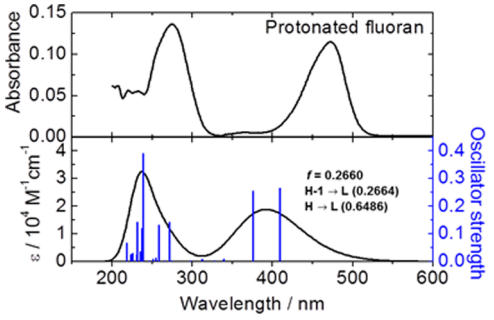

Figure 7. Absorption spectra measured for the fluoran molecule/PC-H_2SO_4 solution (top) and calculated by a TD-DFT method and PCM (RB3LYP 6-31+G(d) basis set): blue bars indicate oscillator strength (bottom). f = oscillator strength, H = HOMO, L = LUMO, and other values are CI coefficients corresponding to the first transition band (409.52 nm).

experimentally obtained one. The calculated excitation energy for the $S_0 \rightarrow S_1$ transition was 409.52 nm (absorption in DMSO), which is close to the experimental result of 465 nm (absorption in PC). This $S_0 \rightarrow S_1$ transition is also fully allowed, as indicated by the overlap between the HOMO−1 or HOMO and LUMO and because f = 0.2660, meaning that the reverse transition, that is, the $S_1 \rightarrow S_0$ transition, is also fully allowed. Thus, the protonated fluoran molecule is fluorescent.

To more intuitively interpret the theoretical calculations, we calculated the fluorescence lifetimes for the neutral and

dx.doi.org/10.1021/jp5060588 | J. Phys. Chem. A XXXX, XXX, XXX−XXX

oxidized fluoran molecules on the basis of the calculated data (Tables S2 and S3,Supporting Information). We used Einstein transition probabilities for the spontaneous transitions, which are described by the following equation:[23]

$$\tau = \frac{C^3}{2(E)^2 f}$$

where τ is the fluorescence lifetime, c stands for the light velocity, E is the transition energy, and f is the oscillator strength. All the parameters are expressed in atomic unit (au).

The calculated fluorescence lifetime was 1498 ns for the neutral fluoran molecule and 9.4 ns for the protonated one undergoing ring opening; thus, the calculated and experimentally obtained lifetimes for the protonated fluoran molecule undergoing ring opening are almost the same. The reasonable calculated and experimentally obtained lifetimes for the protonated fluoran molecule undergoing ring opening indicate that it is fluorescent.[23] The neutral fluoran molecule, however, showed an exceptionally long lifetime, significantly longer than the lifetime range allowed for the relaxation of a singlet excited state (usually the emissive state of most organic fluorophores whose lifetimes are shorter than 10 ns). This long lifetime is a result of nonradiative decay of the excited state.

In this way, the energy gap between S_0 to S_1 (i.e., the absorption wavelength of the molecule) and overlapping of HOMO and LUMO (i.e., transition probability) were effectively controlled by opening and closing of the lactone ring in the fluoran molecule, thereby achieving the switching of both emission and coloration.

CONCLUSION

In summary, we investigated single-molecule switching of both emission and coloration change of the fluoran molecule with molecular structure changes induced by electrochemical or protonation reactions. The fluoran molecule with the closed lactone ring is colorless in the visible region and is practically nonfluorescent under 300 nm excitation. On the other hand, the open state based on protonation with acid or electrochemical reaction showed yellow coloration and green emission upon irradiation of excitation light at 450 nm. This coloration control was induced by the changing of the energy gap between the ground state and the excited states through opening/closing of the lactone ring. Moreover, the photophysical properties corresponding to the different molecular structures in the neutral and oxidized states were clarified by simulating FMOs and applying the DFT theory. From the FMOs, it is clear that nonfluorescent features corresponding to the closed state of the lactone ring are due to the lack of overlap between the HOMO and LUMO, while the fluorescent characteristic corresponding to the open state of lactone ring could be attributed to the significant overlap between the HOMO and LUMO. Thus, the emission of the fluoran molecule could be switched by controlling the overlap between the HOMO and LUMO, and the corresponding change in the IC process after photoexcitation. We expected that this electrochemical switchable molecule will contribute to the development of novel display applications such as rewritable cards, pH indicators, biochemical sensors, and security systems.

ASSOCIATED CONTENT

Supporting Information

Details of absorption spectra, emission spectra, and TD-DFT calculations of neutral and protonated fluoran molecules. This material is available free of charge via the Internet at http://pubs.acs.org.

AUTHOR INFORMATION

Corresponding Authors

*E-mail: Nakamura.Kazuki@faculty.chiba-u.jp (K.N.).
*E-mail: koban@faculty.chiba-u.jp (N.K.).

Notes

The authors declare no competing financial interest.

ACKNOWLEDGMENTS

This work was partly supported by a Grant-in-Aid for Scientific Research (No. 23750208) from the Ministry of Education, Culture, Sports, Science and Technology, Japan, the CASIO Science Promotion Foundation, Inamori Foundation, and JSPS Research Fellowships for Young Scientists. K.K. is a Research Fellow of the Japan Society for the Promotion of Science (JSPS).

REFERENCES

(1) McQuade, D. T.; Pullen, A. E.; Swager, T. M. Conjugated Polymer-Based Chemical Sensors. *Chem. Rev.* **2000**, *100*, 2537−2574.
(2) Martinez-Mañez, R.; Sancenon, F. Fluorogenic and Chromogenic Chemosensors and Reagents for Anions. *Chem. Rev.* **2003**, *103*, 4419−4476.
(3) Rizzo, M. A.; Springer, G. H.; Granada, B.; Piston, D. W. An Improved Cyan Fluorescent Protein Variant Useful for FRET. *Nat. Biotechnol.* **2004**, *22*, 445−449.
(4) De Silva, A. P.; Gunaratne, H. Q. N.; McCoy, C. P. A Molecular Photoionic AND Gate Based on Fluorescent Signaling. *Nature* **1993**, *364*, 42−44.
(5) Credi, A.; Balzani, V.; Langford, S. J.; Stoddart, J. F. Logic Operations at the Molecular Level. An XOR Gate Based on a Molecular Machine. *J. Am. Chem. Soc.* **1997**, *119*, 2679−2681.
(6) De Silva, A. P.; McClenaghan, N. D. Molecular-Scale Logic Gates. *Chem.−Eur. J.* **2004**, *10*, 574−586.
(7) Irie, M. Dialylethene for Memories and Switches. *Chem. Rev.* **2000**, *100*, 1685−1716.
(8) Irie, T.; Fukaminato, T.; Sasaki, T.; Tamai, N.; Kawai, T. A Digital Fluorescent Molecular Photoswitch. *Nature* **2002**, *420*, 759−760.
(9) Wang, X. J.; Lau, W. M.; Wong, K. Y. Display Device with Dual Emissive and Reflective Modes. *Appl. Phys. Lett.* **2005**, *87*, 113502.
(10) Watanabe, Y.; Nakamura, K.; Kobayashi, N. Fabrication of Novel Reflective-Emissive Dual-mode Display Cell Based on Electrochromical Reaction. *Chem. Lett.* **2010**, *39*, 1309−1311.
(11) Audebert, P.; Miomandre, F. Electrofluorochromism: From Molecular Systems to Set-up and Display. *Chem. Sci.* **2013**, *4*, 575−584.
(12) Koyuncu, S.; Usluer, O.; Can, M.; Demic, S.; Icli, S.; Serdar Sariciftci, N. Electrochromic and Electroluminescent Devices Based on a Novel Branched Quasi-Dendric Fluorene-Carbazole-2,5-bis(2-thienyl)-1H-pyrrole. *J. Mater. Chem.* **2011**, *21*, 2684−2693.
(13) Seredyuk, M.; Gaspar, A. B.; Ksenofontov, V.; Reiman, S.; Galyametdinov, Y.; Haase, W.; Rentschler, E.; Gutlich, P. Room Temperature Operational Thermochromic Liquid Crystals. *Chem. Mater.* **2006**, *18*, 2513−2519.
(14) Yoon, S.-J.; Kim, J. H.; Kim, K. S.; Chung, J. W.; Heinrich, B.; Mathevet, F.; Kim, P.; Donnio, B.; Attias, A.-J.; Kim, D.; Park, S. Y. Mesomorphic Organization and Thermochromic Luminescence of Dicyanodistyrylbenzene-Based Phasmidic Molecular Disks: Uniaxially Aligned Hexagonal Columnar Liquid Crystals at Room Temperature

with Enhanced Fluorescence Emission and Semiconductivity. *Adv. Funct. Mater.* **2012**, *22*, 61−69.
(15) Feng, J.; Tian, K.; Hu, D.; Wang, S.; Li, S.; Zeng, Y.; Li, Y.; Yang, G. A Triarylboron-Based Fluorescent Thermometer: Sensitive Over a Wide Temperature Range. *Angew. Chem., Int. Ed.* **2011**, *50*, 8072−8076.
(16) Yan, D. P.; Lu, J.; Ma, J.; Wei, M.; Evans, D. G.; Duan, X. Reversibly Thermochromic, Fluorescent Ultrathin Films with a Supramolecular Architecture. *Angew. Chem., Int. Ed.* **2011**, *50*, 720−723.
(17) Miyata, K.; Konno, Y.; Nakanishi, T.; Kobayashi, A.; Kato, M.; Fushimi, K.; Hasegawa, Y. Chameleon Luminophore for Sensing Temperatures: Control of Metal-to-Metal and Energy Back Transfer in Lanthanide Coordination Polymers. *Angew. Chem., Int. Ed.* **2013**, *52*, 6413−6416.
(18) Hirata, S.; Lee, K.-S.; Watanabe, T. Reversible Fluorescent On−Off Recording in a Highly Transparent Polymeric Material Utilizing Fluorescent Resonance Energy Transfer (FRET) Induced by Heat Treatment. *Adv. Funct. Mater.* **2008**, *18*, 2869−2879.
(19) Nakamura, K.; Kobayashi, Y.; Kanazawa, K.; Kobayashi, N. Thermoswitchable Emission and Coloration of a Composite Material Containing a Europium(III) Complex and a Fluoran Dye. *J. Mater. Chem. C* **2013**, *1*, 617−620.
(20) Fukaminato, T.; Sasaki, T.; Kawai, T.; Tamai, N.; Irie, M. Digital Photoswitching of Fluorescence Based on the Photochromism of Diarylethene Derivatives at a Single-Molecule Level. *J. Am. Chem. Soc.* **2004**, *126*, 14843−14849.
(21) Nakagawa, T.; Hasegawa, Y.; Kawai, T. Nondestructive Luminescence Intensity Readout of a Photochromic Lanthanide(III) Complex. *Chem. Commun.* **2009**, *37*, 5630−5632.
(22) Hasegawa, Y.; Nakagawa, T.; Kawai, T. Recent Progress of Luminescent Metal Complexes with Photochromic Units. *Coord. Chem. Rev.* **2010**, *254*, 2643−2651.
(23) Gingras, M.; Placide, V.; Raimundo, J. M.; Bergamini, G.; Ceroni, P.; Balzani, V. Polysulfurated Pyrene-Cored Dendrimers: Luminescent and Electrochromic Properties. *Chem.−Eur. J.* **2008**, *14*, 10357−10363.
(24) Tropiano, M.; Kilah, N. L.; Morten, M.; Rahman, H.; Davis, J. J.; Beer, P. D.; Faulkner, S. Reversible Luminescence Switching of a Redox-Active Ferrocene−Europium Dyad. *J. Am. Chem. Soc.* **2011**, *133*, 11847−11849.
(25) Wang, B.; Bi, L.-H.; Wu, L.-X. Electroswitchable Fluorescent Thin Film Controlled by Polyoxometalate. *J. Mater. Chem.* **2011**, *21*, 69−71.
(26) Kuo, C.-P.; Chuang, C.-N.; Chang, C.-L.; Leung, M.-k.; Lian, H.-Y.; Wu, K. C.-W. White-light Electrofluorescence Switching from Electrochemically Convertible Yellow and Blue Fluorescent Conjugated Polymers. *J. Mater. Chem. C* **2013**, *1*, 2121−2130.
(27) Nakamura, K.; Kanazawa, K.; Kobayashi, N. Electrochemically Controllable Emission and Coloration by Using Europium(III) Complex and Viologen Derivatives. *Chem. Commun.* **2011**, *47*, 10064−10066.
(28) Kanazawa, K.; Nakamura, K.; Kobayashi, N. Electroswitching of Emission and Coloration with Quick Response and High Reversibility in an Electrochemical Cell. *Chem.−Asian J.* **2012**, *7*, 2551−2554.
(29) Kanazawa, K.; Nakamura, K.; Kobayashi, N. Dual Emissive-Reflective Display Materials with Large Emission Switching Using Highly Luminescent Lanthanide(III) Complex and Electrochromic Material. *Jpn. J. Appl. Phys.* **2013**, *52*, 05DA14/1−4.
(30) Nakamura, K.; Kanazawa, K.; Kobayashi, N. Electrochemically-Switchable Emission and Absorption by Using Luminescent Lanthanide(III) Complex and Electrochromic Molecule Toward Novel Display Device with Dual Emissive and Reflective Mode. *Displays* **2013**, *34*, 389−395.
(31) Jin, L. H.; Fang, Y. X.; Hu, P.; Zhai, Y. L.; Wang, E. K.; Dong, S. J. Polyoxometalate-Based Inorganic−Organic Hybrid Film Structure with Reversible Electroswitchable Fluorescence Property. *Chem. Commun.* **2012**, *48*, 2101−2103.
(32) Gu, H. X.; Bi, L. H.; Fu, Y.; Wang, N.; Liu, S. Q.; Tang, Z. Y. Multistate Electrically Controlled Photoluminescence Switching. *Chem. Soc.* **2013**, *4*, 4371−4377.
(33) Barigelletti, F.; Flamigni, L.; Balzani, V.; Collin, J.-P.; Sauvage, J.-P.; Sour, A.; Constable, E. C.; Cargill Thompson, A. M. W. Rigid Rod-Like Dinuclear Ru(II)/Os(II) Terpyridine-Type Complexes. Electrochemical Behavior, Absorption Spectra, Luminescence Properties, and Electronic Energy Transfer through Phenylene Bridges. *J. Am. Chem. Soc.* **1994**, *116*, 7692−7699.
(34) Jares-Erijman, E. A.; Jovin, T. M. FRET Imaging. *Nat. Biotechnol.* **2003**, *21*, 1387−1395.
(35) Sapsford, K. E.; Berti, L.; Medintz, I. L. Materials for Fluorescence Resonance Energy Transfer Analysis: Beyond Traditional Donor-Acceptor Combinations. *Angew. Chem., Int. Ed.* **2006**, *45*, 4562−4589.
(36) Burkinshaw, S. M.; Griffiths, J.; Towns, A. D. Reversibly Thermochromic Systems Based on pH-Sensitive Functional Dyes. *J. Mater. Chem.* **1998**, *8*, 2677−2683.
(37) Yamamoto, S.; Furuya, H.; Tsutsui, K.; Ueno, S.; Sato, K. In Situ Observation of Thermochromic Behavior of Binary Mixtures of Phenolic Long-Chain Molecules and Fluoran Dye for Rewritable Paper Application. *Cryst. Growth Des.* **2008**, *8*, 2256−2263.
(38) Azizian, F.; Field, A. J.; Heron, B. M.; Kilner, C. Intrinsically Thermochromic Fluorans. *Chem. Commun.* **2012**, *48*, 750−752.
(39) Wang, W.; Higuchi, T.; Suzuki, M.; Fukuoka, T.; Shimomura, T.; Ono, M.; Radhakrishnan, L.; Wang, H.; Suzuki, N.; Oveisi, H.; Yamauchi, Y. A High-Speed Passive-Matrix Electrochromic Display Using a Mesoporous TiO_2 Electrode with Vertical Porosity. *Angew. Chem., Int. Ed.* **2010**, *49*, 3956−3959.
(40) Frisch, M. J.; Trucks, G. W.; Schlegel, H. B.; Scuseria, G. E.; Robb, M. A.; Cheeseman, J. R.; Scalmani, G.; Barone, V.; Mennucci, B.; Petersson, G. A. et al. *Gaussian 09*, rev A.02; Gaussian, Inc.: Wallingford, CT, 2009.
(41) Hohenberg, P.; Kohn, W. Inhomogeneous Electron Gas. *Phys. Rev.* **1964**, *136*, B864−B871.
(42) Kohn, W.; Sham, L. J. Self-Consistent Equations Including Exchange and Correlation Effects. *Phys. Rev.* **1965**, *140*, 1133−1138.
(43) Salahub, D. R.; Zerner, M. C., Eds. *The Challenge of d and f Electrons*; ACS: Washington, DC, 1989.
(44) Parr, R. G.; Yang, W. *Density Fucttional Theory of Atoms and Molecules*; Oxford University Press: Oxford, UK, 1989.
(45) Becke, A. D. Density-Functional Exchange-Energy Approximation with Correct Asymptotic Behavior. *Phys. Rev. A* **1988**, *38*, 3098−3100.
(46) Lee, C. T.; Yang, W. T.; Parr, R. G. Development of the Colle-Salvetti Correlation-Energy Formula into a Functional of the Electron Density. *Phys. Rev. B* **1988**, *37*, 785−789.
(47) Miehlich, B.; Savin, A.; Stoll, H.; Preuss, H. Results Obtained with the Correlation Energy Density Functionals of Becke and Lee, Yang and Parr. *Chem. Phys. Lett.* **1989**, *157*, 200−206.
(48) Becke, A. D. Density-Functional Thermochemistry. III. The Role of Exact Exchange. *J. Chem. Phys.* **1993**, *98*, 5648−5652.
(49) Rassolov, V. A.; Pople, J. A.; Ratner, M. A.; Windus, T. L.; Windus, T. L. 6-31G* Basis set for Atoms K through Zn. *J. Chem. Phys.* **1998**, *109*, 1223−1229.
(50) Bauernschmitt, R.; Ahlrichs, R. Treatment of Electronic Excitations within the Adiabatic Approximation of Time Dependent Density Functional Theory. *Chem. Phys. Lett.* **1996**, *256*, 454−464.
(51) Casida, M. E.; Jamorski, C.; Kasida, K. C.; Salahub, D. R. Molecular Excitation Energies to High-Lying Bound States from Time-Dependent Density-Functional Response Theory: Characterization and Correction of the Time-Dependent Local Density Approximation Ionization Threshold. *J. Chem. Phys.* **1998**, *108*, 4439−4449.
(52) Stratmann, R. E.; Scuseria, G. E.; Frisch, M. J. An Efficient Implementation of Time-Dependent Density-Functional Theory for the Calculation of Excitation Energies of Large Molecules. *J. Chem. Phys.* **1998**, *109*, 8218−8224.
(53) Miertus, S.; Scrocco, E.; Tomasi, J. Electrostatic Interaction of a Solute with a Continuum. A Direct Utilization of Ab Initio Molecular

Potentials for the Prevision of Solvent Effects. *Chem. Phys.* **1981**, *55*, 117−129.
(54) Tomasi, J.; Mennucci, B.; Cammi, R. Quantum Mechanical Continuum Solvation Models. *Chem. Rev.* **2005**, *105*, 2999−3093.
(55) Liou, G. S.; Hsiao, S. H.; Chen, H. W. Novel High-Tg Poly(amine-imide)s Bearing Pendent N-phenylcarbazole Units: Synthesis and Photophysical, Electrochemical and Electrochromic Properties. *J. Mater. Chem.* **2006**, *16*, 1831−1842.
(56) Berridge, R.; Wright, S. P.; Skabara, P. J.; Dyer, A.; Steckler, T.; Argun, A. A.; Reynolds, J. R.; Ross, W. H.; Clegg, W. J. Electrochromic Properties of a Fast Switching, Dual Colour Polythiophene Bearing Non-planar Dithiinoquinoxaline units. *J. Mater. Chem.* **2007**, *17*, 225−231.
(57) Monk, P. M. S.; Mortimer, R. J.; Rosseinsky, D. R. *Electrochromism and Electrochromic Devices*; Cambridge University Press: Cambridge, UK, 2007.
(58) Yang, L.; Ren, A.-M.; Feng, J.-K.; Wang, J.-F. Theoretical Investigation of Optical and Electronic Property Modulations of π-Conjugated Polymers Based on the Electron-Rich 3,6-Dimethoxyfluorene Unit. *J. Org. Chem.* **2005**, *70*, 3009−3020.
(59) Zhang, X.; Chi, L.; Ji, S.; Wu, Y.; Song, P.; Han, K.; Guo, H.; James, T. D.; Zhao, J. Rational Design of d-PeT Phenylethynylated-Carbazole Monoboronic Acid Fluorescent Sensors for the Selective Detection of α-Hydroxyl Carboxylic Acids and Monosaccharides. *J. Am. Chem. Soc.* **2009**, *131*, 17452−17463.
(60) Saita, K.; Nakazono, M.; Zaitsu, K.; Nanbu, S.; Sekiya, H. Theoretical Study of Photophysical Properties of Bisindolylmaleimide Derivatives. *J. Phys. Chem. A* **2009**, *113*, 8213−8220.
(61) Wu, Y.; Guo, H.; Zhang, X.; James, T. D.; Zhao, J. Chiral Donor Photoinduced-Electron-Transfer (d-PET) Boronic Acid Chemosensors for the Selective Recognition of Tartaric Acids, Disaccharides, and Ginsenosides. *Chem.−Eur. J.* **2011**, *17*, 7632−7644.
(62) Turro, N. J. *Modern Molecular Photochemistry*; Benjamin/Cummings Publishing Co.: Merco Park, CA, 1978.
(63) Valeur, B. *Molecular Fluorescence: Principles and Appriations*; Wiley-VCH: Weinhem. Germany, 2002.
(64) Itoh, T. Fluorescence and Phosphorescence from Higher Excited States of Organic Molecules. *Chem. Rev.* **2012**, *112*, 4541−4568.